

IN-BAND PUMPING OF Nd-BASED SOLID-STATE LASERS

NICOLAIE PAVEL

National Institute for Laser, Plasma and Radiation Physics,
Laboratory of Solid-State Quantum Electronics, Bucharest 077125, Romania
email: nicolaie.pavel@inflpr.ro, http://ecs.inflpr.ro/

(Received August 5, 2008)

Abstract. The author is presenting output performances obtained from Nd-based laser materials that were in-band pumped directly into the ${}^4F_{3/2}$ emitting level. Continuous-wave (cw) laser operation at 1.06 μm with slope efficiency of 0.79 in Nd:YAG and 0.80 in Nd:GdVO₄ and Nd:YVO₄ was realized using an end-pumping configuration and a tunable Ti:Sapphire laser around 0.88 μm as source of excitation. These slopes are very close to the limits of the investigated laser materials. Laser operation at 0.946 μm in Nd:YAG with slope efficiency as high as 0.68 was also demonstrated. The influence of an increased Nd concentration on the quantum efficiency of the ${}^4F_{3/2}$ emitting level in Nd:YAG is discussed, and laser performances at 1.06 μm in highly-doped Nd laser are investigated. Laser emission at 1.3 μm was demonstrated for the first time in a highly-doped 2.5 at % Nd:YAG under pumping with diode lasers at 0.88 μm . First diode end-pumped at 0.88 μm Nd:GdVO₄ laser that generated 5.1 W of green at 0.53 μm visible light by intracavity frequency doubling was realized. The pump at 0.88 μm was also employed with active medium in thin-disk geometry. A multi-pass pumped Nd:GdVO₄ laser with cw maximum output power of 14.9 W at 1.06 μm and that generated 9.1 W of green light at 0.53 μm was demonstrated.

Key words: lasers and laser optics; lasers, solid-state; lasers, diode-pumped; lasers, neodymium; thermal effects; pumping; visible lasers; frequency conversion.

1. INTRODUCTION

The first diode-pumped Nd solid-state lasers were demonstrated using in-band pumping directly into the ${}^4F_{3/2}$ upper level. Thus, radiation at 880 nm from GaAs diodes was used to excite the 1.06 μm fluorescence spectrum of Nd:CaWO₄ [1], and diodes with emission at 869 nm were employed to demonstrate the first transverse- and end-pumped Nd:YAG lasers [2, 3]. The choice of the pump into the ${}^4F_{5/2}$ level at $\sim 0.81 \mu\text{m}$, which is now used commonly to realize Nd lasers, was determined by a stronger absorption of the pump radiation in this range and by the availability of suitable diode lasers. The quantum defect ratio, η_{qd} (*i.e.* the ratio

between the pump wavelength, λ_p and the emission wavelength, λ_{em}) is, however, a major limitation in power scaling of a solid-state laser. Various parameters of the laser emission (absorbed pump power at threshold, slope efficiency or optical efficiency), are influenced by η_{qd} , which also has a major contribution to the heat generated in the laser medium. Thus, reduction of the quantum defect, $(1 - \eta_{qd})$ is an important issue for optimization of laser performances, and for Nd laser materials this can be realized by using in-band pumping directly into the ${}^4F_{3/2}$ emitting level.

The research on this subject was revitalized after the year 1999. Laser performances at 1064 nm in Nd:YAG pumped at 869 nm and at 885 nm [4, 5], and in Nd:YVO₄ pumped at 880 nm [5] were investigated by a team from Israel, by using as pump source a tunable Ti:Sapphire laser. An increase of the slope efficiency with respect to the absorbed pump power, η_{sa} by 5 to 12% and a decrease of the absorbed pump power at threshold, $P_{th,a}$ by 11% were recorded for the in-band pumping, compared with the pump into the ${}^4F_{5/2}$ level. In 2001, a Nd:YAG laser with 14 W cw output power at 1064 nm and an overall optical-to-optical efficiency, η_o of 0.53 was reported by the same research group under pump with diode lasers at 885 nm [6]; the slope efficiency with respect to the incident pump power, η_s was 0.63. The first demonstration of laser emission on the quasi-three-level ${}^4F_{3/2} \rightarrow {}^4I_{9/2}$ transition at 914 nm in Nd:YVO₄ under pump at 880 nm was reported in 1999 by a research group from Hamburg University, Germany [7]. In this case, the pump with a Ti:Sapphire laser yielded a slope efficiency η_{sa} of 0.51. In 2002 a research team from USA employed diode lasers with emission at 880 nm to realized a Nd:YVO₄ laser with an output power of 10.8 W at 1064 nm for 24 W of absorbed pump power, P_{abs} [8]. In all these experiments the optical excitation was made in an end-pumping scheme. Therefore, good absorption of the pump radiation was realized by using long active media, with a length between 12 and 40 mm [4–6, 8]. However, such a laser configuration has a lower than unity spatial overlap efficiency between the pump and laser beam volumes, η_m and an increased round-trip residual losses L_i , which limits the laser performances at 1.06 μm . Moreover, lengthening the laser crystal will increase the reabsorption losses, which is detrimental for achieving efficient laser emission on the quasi-three-level ${}^4F_{3/2} \rightarrow {}^4I_{9/2}$ transition at 0.9 μm in these materials.

In this work I review results on laser emission at 0.9, 1.06 and 1.3 μm obtained from Nd-based laser crystals that were in-band pumped directly into the ${}^4F_{3/2}$ emitting level. Two laser configurations were investigated. First, the end-pumping scheme with a Ti:Sapphire laser of highly-doped laser crystals with a thickness of a few millimeters was employed to demonstrate laser emission at 1.06 μm with slopes efficiencies η_{sa} as high as 0.79 in Nd:YAG, and 0.80 in

Nd:YVO₄ and Nd:GdVO₄. For the first time laser emission at 0.946 μm is demonstrated in Nd:YAG using the pump at 0.885 μm with a Ti:Sapphire laser as well as with diode lasers, and high-power emission at 1.3 μm is achieved in low and highly-doped Nd:YAG under pump with diode lasers. The in-band pump is used to improve also the performances of Nd-lasers with generation into visible spectrum by intracavity-frequency doubling. An LiB₃O₅-Nd:GdVO₄ laser with cw high output power into visible spectrum at 0.53 μm is realized for the first time. Secondly, the thin-disk geometry of the laser crystal and multi-pass pumping were the solutions used to obtain improved output performances at 0.91 and 1.06 μm from Nd:GdVO₄ and Nd:YVO₄ crystals that were in-band pumped with diode lasers. Nd-vanadate lasers with cw output power in excess of 10 W at 1.06 μm, and in the watt range at 0.91 μm were demonstrated in this scheme, for the first time. Intracavity frequency doubling allowed realization of a cw Nd:GdVO₄ thin-disk laser with 9.1 W output power of green light at 0.53 μm, and of a Nd:YVO₄ thin-disk laser with 1.0 W output power into ‘deep-blue’ at 0.456 μm visible range. Comparative results with the pump at 0.81 μm into the highly absorbing ⁴F_{5/2} level are presented, proving the advantage of the in-band directly into the emitting ⁴F_{3/2} level pumping.

2. RESULTS AND DISCUSSION

2.1. SPECTROSCOPIC PROPERTIES

Fig. 1a presents the diagram of the energy levels in Nd:YAG. The strongest line in the ⁴I_{9/2} → ⁴F_{3/2} absorption spectrum at room temperature corresponds to the Z₁ → R₂ transition at 869.9 nm (Fig. 1b). However, this line has a spectral bandwidth Δλ below 1 nm (FWHM definition), and is therefore less suitable for pumping with diode lasers. Promising is the double-peaked absorption band centered on 885 nm that collects the thermally activated lines Z₂ → R₁ (885.7 nm) and Z₃ → R₂ (884.3 nm) of the ⁴I_{9/2} → ⁴F_{3/2} absorption. The absorption coefficients of the two peaks are almost equal, ~ 1.7 cm⁻¹ for 1 at %, ~ 6.5 cm⁻¹ for 4 at %, and 13 to 14 cm⁻¹ for 9 at % Nd, whereas that corresponding to the dip between the peaks is about 15% lower. These peak absorption coefficients are almost half of that of the Z₁ → R₂ transition. However, the width Δλ for the 885 nm band is ~ 2.5 nm for 1 at % and ~ 3.2 nm for 9 at % Nd, which is more than three times larger than for the 869.9 and 808.7 nm lines, and comparable with the emission width of available diode lasers. The pump directly into the ⁴F_{3/2} level changes the quantum defect ratio η_{qd} from 0.76 for the pump at 809 nm to 0.83 for

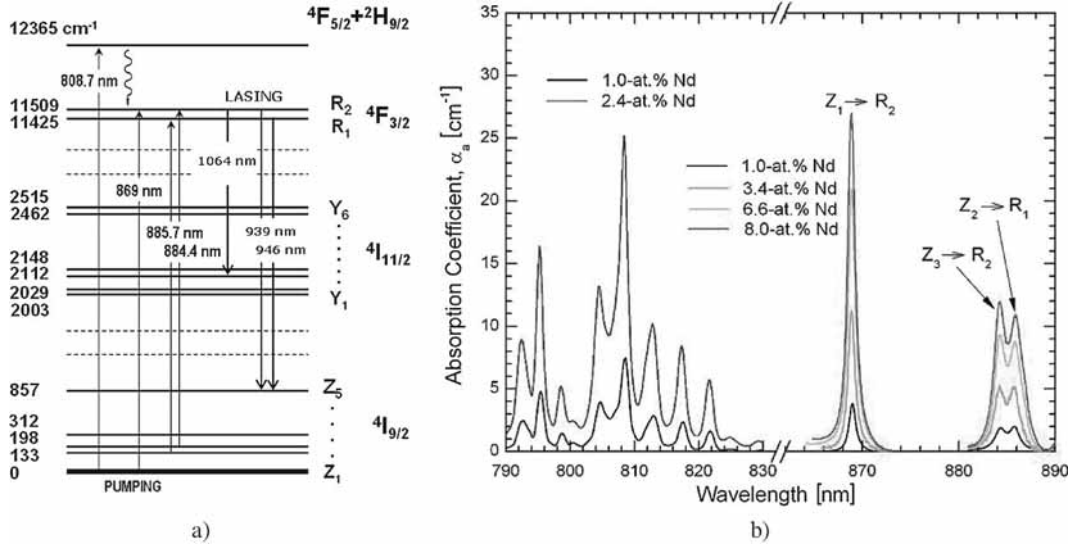


Fig. 1 – a) Diagram of the energy levels of Nd:YAG with a description of the pump into the highly-absorbing ${}^4F_{5/2}$ level and of the in-band into the ${}^4F_{3/2}$ upper level pumping; b) ${}^4I_{9/2} \rightarrow {}^4F_{5/2}$ and ${}^4I_{9/2} \rightarrow {}^4F_{3/2}$ absorption coefficient at room temperature of Nd:YAG at various doping levels.

the pump at 885 nm in the case of $\lambda_{em} = 1064$ nm, and from 0.855 to 0.936 for the emission at $\lambda_{em} = 946$ nm. This induces a reduction of the fractional thermal load, η_h . For example, η_h is reduced by $\sim 29\%$ in the case of efficient laser emission at 1064 nm, from 0.24 to 0.17.

On the other hand, an increase of Nd concentration (C_{Nd}) influences the population dynamics of the excited states and changes the emission quantum efficiency, η_{qe} (*i.e.* the fraction of the ions from the metastable ${}^4F_{3/2}$ level that deexcite radiatively in the absence of laser emission). Fig. 2a presents the variation of η_{qe} with C_{Nd} in the case of Nd:YAG. The continuous line is the calculus of η_{qe} from the emission decay, based on a theory described in Refs. [9–11]. Modeling shows a good agreement with the experimental data recorded by different methods, such as decay kinetics of the ${}^4F_{3/2}$ level [12], heat generation [13], or thermally induced birefringence [14]. The reduction of efficiency η_{qe} with increased C_{Nd} would induce an increase in the emission threshold. However, due to the proportionality of the absorption coefficient α_a to C_{Nd} , the negative effect of decreasing η_{qe} at high C_{Nd} can be compensated by an increased absorption efficiency, η_a of the pump radiation.

When the product $\eta_{qe}C_{Nd}$ is taken as a figure of merit for the laser potential of the concentrated Nd:YAG materials, one could see that this parameter is larger than for the 1.0 at % Nd up to C_{Nd} around 8.5 at % Nd, with a maximum in the region

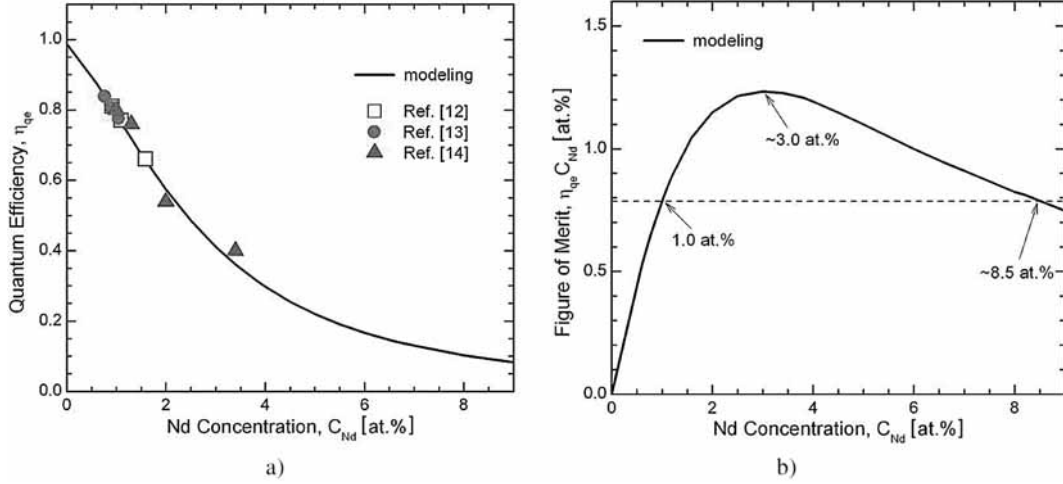


Fig. 2 – a) The variation of the emission quantum efficiency, η_{qe} on C_{Nd} ; b) the figure of merit $\eta_{qe}C_{Nd}$ for the ${}^4F_{3/2}$ laser level in Nd:YAG. Signs are experimental data according to Ref. [12] (\square), Ref. [13] (\diamond), and Ref. [14] (\blacktriangle).

region of 3 at % Nd, as shown in Fig. 2b. The efficiency η_{qe} does not influence the slope efficiency η_s , whereas the increased absorption η_a at high C_{Nd} increases the slope η_s . This indicates that concentrated Nd:YAG materials can be used for construction of efficient solid-state lasers in free-generation or low storage regimes.

Principal spectroscopic characteristics of Nd:YAG, Nd:YVO₄ and Nd:GdVO₄ laser materials are given in Table 1. The main laser emission in the 1 μ m range in Nd:YVO₄ is at 1064.2 nm, and is based mainly on the transition $R_1 \rightarrow Y_1$ with weak contribution from transition $R_2 \rightarrow Y_2$. The effective emission cross-section, σ_{em} for π polarization at this wavelength is about four times larger than for the

Table 1

Spectroscopic properties of Nd:YAG, Nd:YVO₄ and Nd:GdVO₄

Medium	Emission, $\sigma_{em} (\times 10^{-19} \text{ cm}^2)$			Absorption, $\sigma_{abs} (\times 10^{-19} \text{ cm}^2)$		Lifetime $\tau_f (\mu\text{s})$ (1.0 at % Nd)	Emission quantum efficiency, η_{qe}		
	${}^4F_{3/2} \rightarrow {}^4I_{1/2}$ ($\lambda_{em} = 1.06 \mu\text{m}$)	$\sigma_{1.06\mu\text{m}}/$ $\sigma_{1.34\mu\text{m}}$	$\sigma_{1.06\mu\text{m}}/$ $\sigma_{0.9\mu\text{m}}$	${}^4I_{9/2} \rightarrow {}^4F_{3/2}$ ($l_p = 0.80 \mu\text{m}$)	$\sigma_{0.88\mu\text{m}}/$ $\sigma_{0.80\mu\text{m}}$		C_{Nd} (at %)		
						1.0	2.0	3.0	
Nd:YAG	2.9	~ 5.0	~ 7.4	0.79	~ 0.12	228	0.78	0.57	0.41
Nd:YVO ₄	12.3 (π) 5.2 (σ)	~ 3.3 (π)	25.6 (π) 12.1 (π)	6.0 (π) 1.2 (σ)	~ 0.70	84	0.715	0.39	0.24
Nd:GdVO ₄	12.5 (π) 6.1 (σ)	~ 4.2 (π)	18.9 (π) 10.9 (π)	5.4 (π) 1.2 (σ)	~ 0.50	83	–	–	–

1064.15 nm emission in Nd:YAG. Although the lifetime τ_f of the ${}^4F_{3/2}$ level in Nd:YVO₄ is by about three times shorter than in YAG, the product $\tau_f\sigma_{em}$ is larger in the former, determining a lower threshold of emission. In case of Nd:YVO₄, the strongest line in the ${}^4I_{9/2} \rightarrow {}^4F_{3/2}$ absorption spectrum corresponds to transition $Z_1 \rightarrow R_1$ at 879.6 nm, whose cross-section is about 70% of that for ${}^4I_{9/2} \rightarrow {}^4F_{5/2}$ transition, whereas the line-widths are similar (~ 1.5 nm). In the case of Nd:GdVO₄, the most intense transition in the room-temperature ${}^4I_{9/2} \rightarrow {}^4F_{3/2}$ absorption spectrum, at 879.1 nm, originates from the first Stark component Z_1 of the ground manifold ${}^4I_{9/2}$. The peak absorption cross section of this transition is $\sim 2.7 \times 10^{-19}$ cm², about half that of the 808 nm pump, while the absorption width $\Delta\lambda$ of ~ 2.3 nm is larger [15]. An additional advantage of Nd:GdVO₄ is the quasi-degeneracy of the two Stark components of emitting level ${}^4F_{3/2}$: Thus, all the population of this level is used for laser emission.

2.2. CHARACTERISTICS OF LASER EMISSION OBTAINED IN THE END-PUMPING SCHEME

The cw laser emission at $\lambda_{em} = 1.06$ μ m of the Nd laser materials employed in our experiments were first investigated using as pump source a tunable Ti:Sapphire laser. One side of each laser crystal was coated as antireflection (AR) for λ_{em} and high-transmission (HT) for the pump wavelength λ_p around 0.81 and 0.88 μ m, whereas the second side was AR coated for λ_{em} . A rotating polarizer was used to vary the pump power that was incident upon the crystal, and to keep unchanged the Gaussian distribution of the pump beam. The Nd crystals were mounted in a copper holder whose temperature was controlled by a Peltier element, and an indium foiled was placed between the crystal and the holder in order to decrease the thermal impedance. The pump beam was focused on the laser crystals to a spot of 50 μ m in diameter. A plane-concave resonator of 30 mm length and an output mirror with 50 mm radius of curvature and transmission, T at λ_{em} from 0.01 to 0.20 was used.

Fig. 3 presents the best performances achieved in these experiments. In the case of Nd:YAG (1.0 at % Nd, thickness of 3 mm), the slope efficiency η_{sa} under the pump at 885 nm (directly into the ${}^4F_{3/2}$ emitting level) was 0.79 (Fig. 3a), and the absorbed pump power at threshold was $P_{th,a} \sim 25$ mW. The maximum output power at 1064 nm was 0.32 W for an absorbed pump power $P_{abs} = 0.43$ W, which corresponds to an optical efficiency η_{oa} of about 0.74. In the case of the pump at 809 nm (into the highly absorbing ${}^4F_{5/2}$ level), the slope η_{sa} decreased at 0.70, and the threshold $P_{th,a}$ increased at ~ 70 mW. Due to an improved absorption η_a (from

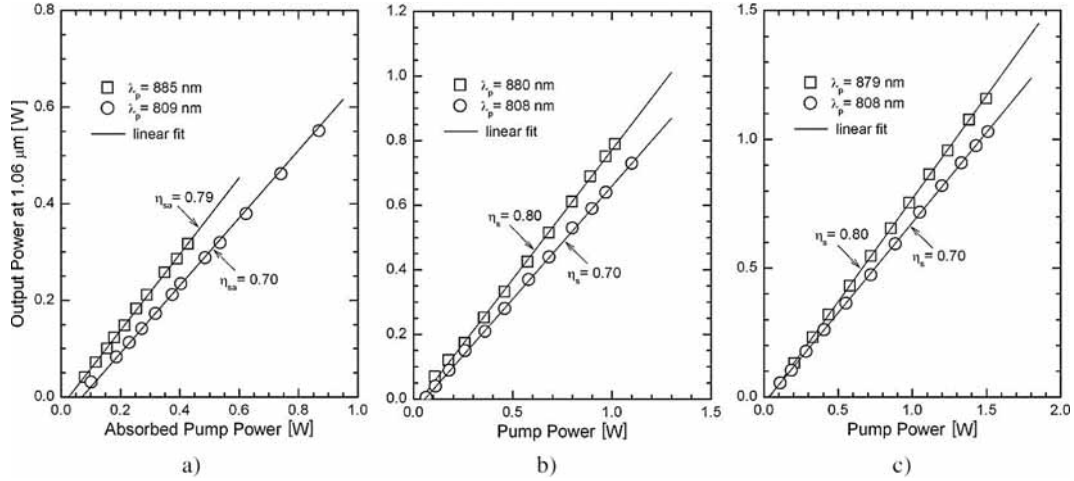


Fig. 3 – Output performances at 1.06 μm achieved under pumping with a Ti:Sapphire laser into the $^4F_{5/2}$ and $^4F_{3/2}$ levels of: a) Nd:YAG; b) Nd:YVO₄; c) Nd:GdVO₄.

$\eta_a = 0.25$ for the pump at 885 nm to $\eta_a = 0.83$ for the pump at 809 nm), the maximum output power increased at 0.55 W for $P_{\text{abs}} = 0.87$ W ($\eta_{\text{oa}} = 0.63$). These results were recorded with an output mirror of transmission $T = 0.10$.

In the case of Nd-vanadate crystals the pump was made along the Ellc axis (*i.e.* π polarization). The Nd:YVO₄ crystal was a 1-mm thick, a-cut plate with 1.0 at % Nd that absorbed almost all the incident pump power. As shown in Fig. 3b, the slope efficiency η_s was 0.80 for the pump at $\lambda_p = 880$ nm. The maximum output power at 1064 nm was 0.79 at an incident pump power of 1.0 W (overall optical efficiency $\eta_o = 0.79$). The Nd:GdVO₄ crystal (1.0 at % Nd, thickness of 3 mm) yielded 1.16 W at 1063 nm for 1.5 W of incident pump power at 879 nm ($\eta_o \sim 0.77$). Again, the slope efficiency η_s reached 0.80 (Fig. 3c). For the Nd-vanadates crystals the pump at 808 nm resulted in laser operation with a slope efficiency η_s as high as 0.70. In these experiments the output mirror has a transmission $T = 0.20$.

The pump at 0.88 μm , directly into the $^4F_{3/2}$ emitting level resulted in laser emission at 1.06 μm with slope efficiencies that were very close of the quantum defect ratio η_{qd} (0.83 for Nd:YAG and ~ 0.827 for Nd vanadates). The data gave consistently round-trip residual losses L_i close of 0.01 for all the investigated laser crystals, with the spatial overlap η_m close to unity. Thus, the difference between the obtained slope efficiency and those determined by η_{qd} for these wavelengths of pump could be fully accounted by the residual optical losses L_i [16–18].

Based on availability, the output power at 1.06 μm was measured for various highly-doped Nd crystals that were in-band pumped at $\lambda_p = 0.88$ μm . For example,

with an output mirror of $T = 0.10$, a coated 2.4 at % Nd:YAG crystal of 3 mm thickness emitted with a slope efficiency $\eta_{sa} = 0.70$ (Fig. 4). The increased absorption efficiency at 885 nm, $\eta_a \sim 0.61$ compared with $\eta_a \sim 0.25$ of the 1.0 at % Nd:YAG, yielded an maximum output power of 0.58 W at $P_{abs} = 0.87$ W ($\eta_{oa} \sim 0.67$). Furthermore, a coated 3.5 at %, 1.0 mm thick Nd:YAG crystal emitted with a slope efficiency $\eta_{sa} = 0.46$. The most concentrated Nd:YAG component that lased was an uncoated, 0.4 mm-thick ceramics of 6.8 at % Nd: The slope efficiency was $\eta_{sa} = 0.20$ for the pump at 885 nm. The laser emission parameters in absorbed power obtained under the pump at 808 nm for these Nd:YAG samples were by 9 to 14% lower than those recorded for the pump at 885 nm.

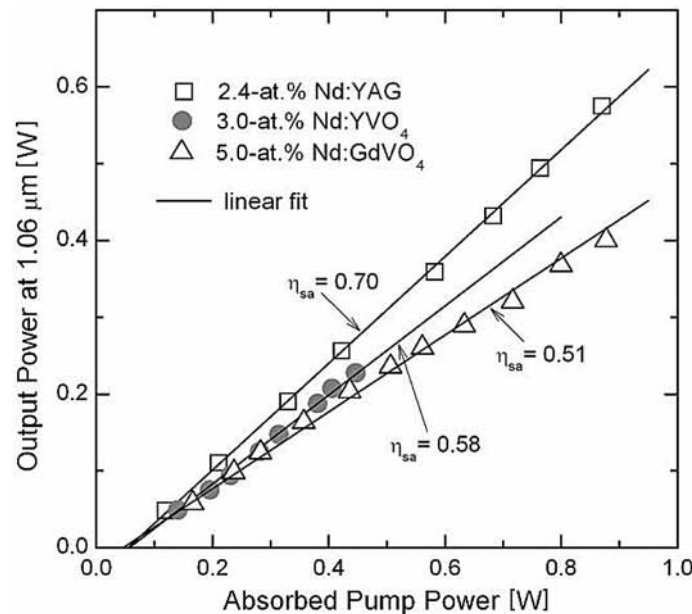


Fig. 4 – The output power at 1.06 μm vs. the absorbed pump power at 0.88 μm measured from highly-doped Nd-laser crystals: 2.4 at %, 3 mm thick Nd:YAG, coated sample; 3.0 at %, 0.9 mm thick, uncoated Nd:YVO₄; and 5.0 at %, 1.2 mm thick, uncoated Nd:GdVO₄.

Highly-doped, uncoated, a-cut Nd-vanadates crystals were also tested in the experiments. A 3.0 at %, 0.9 mm thick Nd:YVO₄ delivered 0.23 W at 1064 for $P_{abs} = 0.48$ W at 880 nm, and an output mirror with $T = 0.05$. The overall efficiency η_{oa} and the slope efficiency η_{sa} were 0.48 and 0.58 respectively. Laser emission could be observed only around the threshold for the pump at 808 nm of this Nd:YVO₄ crystal, most probably due to a severe heating of the sample. In the case of a Nd:GdVO₄ crystal (5.0 at % Nd, 1.2 mm thick), laser emission with slope

efficiency $\eta_{sa} = 0.51$ was recorded for the pump at 879 nm. The maximum output power at 1063 nm was 0.4 W with $\eta_{oa} \sim 0.45$. The slope efficiency η_{sa} decreased at 0.30 for the pump at 808 nm, and a fast decrease of the output power was observed for absorbed pump powers in excess of 0.75 W.

The quasi-three-level 946 nm emission of Nd^{3+} in YAG is important for construction of solid-state lasers at the fundamental frequency, or for doubling it by nonlinear processes to the blue 473 nm light. The 946 nm cw laser emission in a 1.0 at %, 3 mm thick Nd:YAG crystal was investigated using the pump at 809 and 885 nm with a tunable Ti:Sapphire laser. The 3 crystal was HT coated for λ_p of 808 and 885 nm, and AR coated for $\lambda_{em} = 946$ nm. A plane-concave resonator of 25 mm length and an output mirror of 50 mm radius were employed. The Ti:Sapphire laser was focused on the active component in a 160 μm diameter spot. Fig. 5 shows the output performances at 946 nm. For the pump at 885 nm, the best results were obtained with an output mirror of $T = 0.03$. The absorbed pump power at threshold is $P_{th,a} = 0.12$ W, and the slope efficiency at P_{abs} about four times larger than the threshold reaches $\eta_{sa} = 0.68$. This is the highest slope efficiency obtained for cw 946 nm laser emission in Nd:YAG [19]. An output power of 0.18 W resulted for $P_{abs} = 0.50$ W at 885 nm. In the case of $\lambda_p = 809$ nm, the

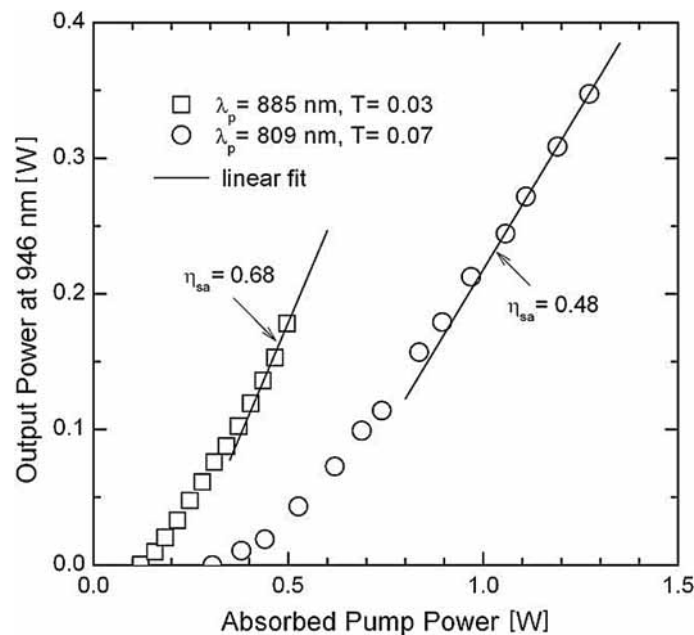


Fig. 5 – The output power at 946 nm vs. the absorbed pump power at 809 and 885 nm obtained from a 3 mm thick, 1.0 at % Nd:YAG laser crystal.

highest slope η_{sa} at P_{abs} of about four times the threshold was 0.48, for an output mirror with $T = 0.07$. It can be observed that under 808 nm pumping, the emission threshold is larger and the slope efficiency is smaller than for the pump at 885 nm. I mention that in 2006 the first demonstration of a laser emission at 946 nm in Nd:YAG under pumping with diode lasers at 885 was made [20]. The device yielded cw 1 W output power for $P_{abs} = 4$ W (which corresponds to $\eta_{oa} = 0.25$), at a slope efficiency $\eta_{sa} = 0.49$.

The laser performances of the ${}^4F_{3/2} \rightarrow {}^4I_{13/2}$ transition at 1.3 μm in Nd:YAG were measured under end-pumping with diode lasers [20, 21]. A 3 mm thick, 1.0 at % Nd:YAG crystal and a highly-doped 2.5 at % Nd:YAG crystal (thickness of 5 mm) were used in the experiments. Both crystal surfaces were AR coated at $\lambda_{em} = 1.3$ μm and HT coated for λ_p of 807 and 885 nm. The crystals were wrapped in indium foil and clamped in a copper holder, whose temperature was kept at 18°C. The pump at 807 nm was made with a 400 μm diameter, 0.22 NA fiber-coupled diode (LIMO Co., Germany), with a maximum power of 32 W in a FWHM spectrum width of $\Delta\lambda \sim 2.5$ nm. The pump into the ${}^4F_{3/2}$ emitting level was performed with an 885 nm diode laser (Hamamatsu K.K., Japan), with the same fiber characteristics as the 807 nm diode. This diode emitted 20 W at the fiber end in a spectrum of $\Delta\lambda \sim 2.5$ nm. A 1:1 optical system was used to image the fiber end into the laser crystal. A plane-concave resonator of 45 mm length with an output mirror of 100 mm radius was employed. The Nd:YAG component was placed close of the plane mirror, which was HR coated at $\lambda_{em} = 1.34$ μm and HT coated for the pumping wavelengths.

The best performances were obtained with a $T = 0.03$ output mirror, as shown in Fig. 6. In the case of the pump at 807 nm, the 1.0 at % Nd:YAG crystal emitted 3.1 W power for $P_{abs} = 9.3$ W ($\eta_{oa} = 0.33$), with slope $\eta_{sa} = 0.37$ and 0.62 W absorbed pump power at threshold (Fig. 6a). Output power saturation was observed for P_{abs} in excess of ~ 9.5 W, which suggests strong thermal effects in Nd:YAG at this lasing wavelength. The 2.5 at % Nd:YAG emitted 2.5 W at 1.34 μm for $P_{abs} = 10.8$ W, with decreased optical efficiency η_{oa} and slope efficiency η_{sa} of 0.23 and 0.27, respectively. The output power decreased beyond this pumping level (Fig. 4a).

This behavior was not observed under in-band pumping at 885 nm (Fig. 6b). A maximum output power of 1.3 W was measured from the 1.0 at % Nd:YAG at $P_{abs} = 3.5$ W. The threshold was $P_{th,a} = 0.60$ W and the slope efficiency η_{sa} achieved 0.45. Moreover, in the case of highly-doped 2.5 at % Nd:YAG crystal the slope efficiency was $\eta_{sa} = 0.39$, and the output power reached 3.8 W for $P_{abs} = 10.3$ W (*i.e.* $\eta_{oa} = 0.37$). The laser emission characteristics were influenced by a specific degradation of the optical quality of the laser media at high C_{Nd} . However,

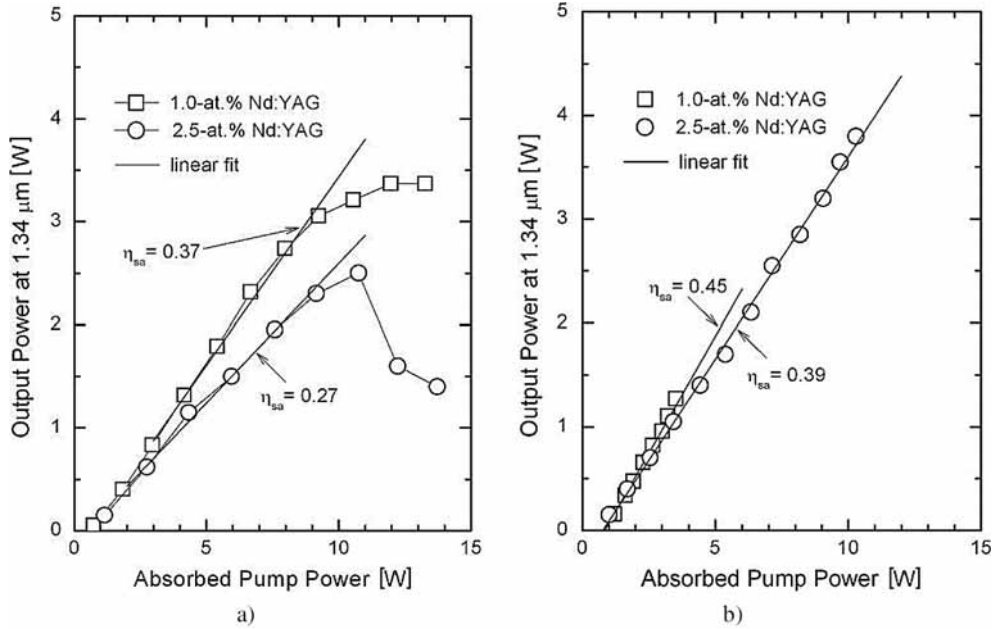


Fig. 6 – The output power at 1.34 μm vs. the absorbed pump power recorded from 1.0 and 2.5 at % Nd:YAG laser crystals that were end-pumped with diode lasers at: a) 807 nm; b) 885 nm.

progress in improving this quality gives hope that this problem could be solved in the future.

The influence of lasing wavelength λ_{em} and medium concentration C_{Nd} on the thermal effects induced by optical pumping into the active component was also investigated. It was concluded that, compared with the non-lasing regime, efficient laser emission at 1.3 μm increases the thermal effects in the laser material for Nd doping below $C_{Nd} \sim 1.14$ at %. Above this value the thermal effects under efficient lasing becomes smaller than those under non-lasing. This behavior was checked by mapping the temperature of the output surface of the Nd:YAG crystals.

In the previous experiments, the in-band pump around 0.88 μm into the ${}^4F_{3/2}$ emitting level was demonstrated to improve the laser performances with respect to the absorbed pump power, in comparison with the pump at 0.81 μm into the ${}^4F_{5/2}$ level. Therefore, our next task was realization of in-band pumped Nd-lasers whose output characteristics with respect to the incident pump power could compete with those of the same laser pumped at 0.81 μm. Moreover, as suggested and demonstrated for the first time by V. Lupei *et al.* [17], the pump directly into the emitting level can improve also the performances of lasers that generate visible light by intracavity frequency-doubling. As solutions to this quest we used two approaches: i) end-pumping of highly-doped Nd-vanadates, and ii) multi-pass pumping of Nd-vanadate thin-disk laser crystals. The results obtained with the first

approach will be described next, whereas Section 2.3 will presents the data obtained with thin-disk geometry of the laser medium.

The experimental set-up that was designed for 1.06 μm emission in Nd:GdVO₄ is shown in Fig. 7a. The 3 mm thick, 1.0 at % Nd:GdVO₄ crystal has the side S1 coated as AR for λ_p of 808 and 879 nm and as HR for $\lambda_{em} = 1063$ nm. The opposite side S2 was AR coated for λ_{em} and HR coated for both λ_p . The optical pumping was made with the same diode lasers described previously. A folded Z-type resonator that realized a good laser-to-pump beam overlap efficiency, η_m and that was characterized by a low sensitivity to the thermal effects induced by optical pumping into the Nd:GdVO₄ crystal was build. The resonator length was 120 mm and it consisted of two mirrors M1 and M2, both of 500 mm radius, that were HR coated at λ_{em} . A plane mirror, M3 was used as the output mirror. The intracavity frequency-doubling set-up is shown in Fig. 7b The green generation at 0.53 μm was obtained with a 10 mm long LiB₃O₅ (LBO) nonlinear crystal that was cut for type I critical phase-matching ($\theta = 90^\circ$, $\phi = 11.4^\circ$) and that was operated at 25°C. The plane mirror M3 and the 500 mm radius mirror M2 were HR coated at 0.53 and 1.06 μm . Mirror M1 (radius of 500 mm) was used to couple the green radiation out of the laser cavity, being therefore HR coated at λ_{em} and HT coated at 0.53 μm .

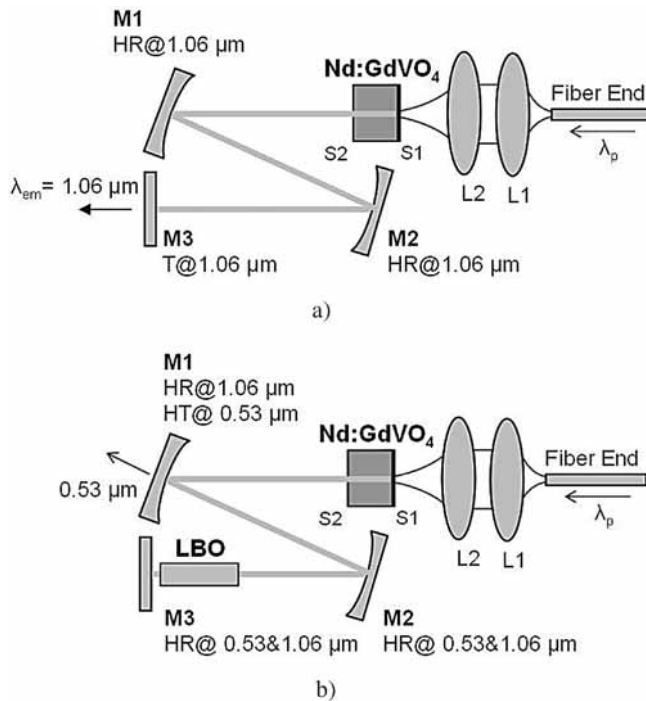


Fig. 7 – A sketch of the diode end-pumped Nd:GdVO₄ laser operating at: a) the fundamental wavelength of 1.06 μm ; b) generation of green at 0.53 μm light by intracavity frequency doubling with LBO non-linear crystal. L: lenses; M1, M2, M3: mirrors.

Fig. 8 presents the output performances at 0.53 and 1.06 μm of the end-pumped Nd:GdVO₄ laser. The pump at 808 nm delivered 8.9 W output power at 1063 nm for an input pump power of 16.5 W, which corresponds to an optical efficiency η_o of 0.54. The slope efficiency η_s was 0.57. (Fig. 8a). The mirror M3 has transmission $T = 0.10$ at the lasing wavelength. In the case of pump into the $^4F_{3/2}$ emitting level, the laser outputted 8.3 W at 1.63 nm for an input pump power of 16.7 W at 879 nm ($\eta_o = 0.50$); the slope efficiency was $\eta_s = 0.50$ (Fig. 8b). A prove of a lower heat generated in the Nd:GdVO₄ crystal under the in-band pump was the M^2 factor of the laser beam. For the maximum output power, the M^2 factor was 2.76 for the pump at 808 nm, and improved at 1.38 for the pump at 879 nm.

The maximum power at 0.53 μm under the pump at 808 nm was 4.4 W with an optical efficiency η_o of nearly 0.27. The beam M^2 factor was 3.40. Saturation of the green-light power was observed for P_{in} in excess of 10 W. When the Nd:GdVO₄ laser was pumped at $\lambda_p = 879$ nm, the maximum power of the green light increased at 5.1 W, with the optical efficiency $\eta_o = 0.30$. The beam M^2 factor improved to 1.46, compared with the pump at 808 nm. This was the first demonstration of a Nd:GdVO₄ laser pumped directly into the emitting level, and that was intracavity frequency-doubled to obtain generation of visible light at 0.53 μm [22].

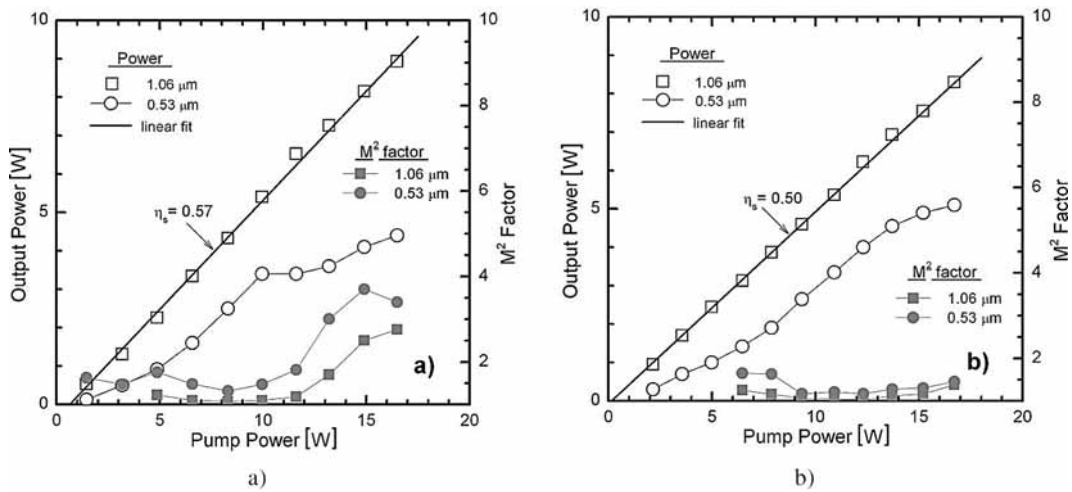


Fig. 8 – The output power at 0.53 and 1.06 μm and M^2 factor of the laser beams obtained from the 1.0 at % Nd:GdVO₄ crystal pumped with diode lasers at: a) 808 nm; b) 879 nm.

2.3. Nd-VANADATES IN THIN-DISK GEOMETRY

The multi-pass pumped thin-disk architecture has been proved to be extremely suitable for Yb:YAG [23, 24]. The first demonstration of a thin-disk

laser pumped directly into the ${}^4F_{3/2}$ emitting level, which used Nd:GdVO₄, was made in 2005 [25]. This laser emitted 3.6 W output power at 1063 nm for an absorbed pump power $P_{\text{abs}} = 6.9$ W at 879 nm ($\eta_{\text{oa}} = 0.52$) with a slope efficiency $\eta_{\text{sa}} = 0.69$. However, because a pumping scheme with only 4 passes of the thin-disk crystal was used, the absorption efficiency η_{a} was limited at 0.34. The absorption η_{a} and the optical efficiency η_{o} can be improved by increasing the number of the passes through the medium, for example by using a parabolic mirror [26, 27].

A sketch of the experimental set-up is shown in Fig. 9a. The laser crystals used in the experiments were 0.5 at % Nd:GdVO₄ and 0.3 at % Nd:YVO₄, with a thickness of 300 μm . One side of the medium (S1) was coated for HR at the pump wavelengths λ_{p} (0.81 and 0.88 μm) and at the lasing wavelength of $\lambda_{\text{em}} = 1.06$ μm . The second side of the crystal (S2) was coated for HT at λ_{p} and as AR at λ_{em} . The laser medium was attached with side S1 to a copper heat sink by using a metallic-soldering technique based on indium and tin. The optical pumping at 0.88 μm was made with a fiber-coupled diode laser of DILAS Co., Germany. The maximum cw output power delivered by this diode was 30 W and the emission spectrum width was $\Delta\lambda_{\text{p}} \sim 3.0$ nm. For the pump at 0.81 μm a fiber-coupled diode laser of Jenoptik, Germany (JOLD30-CPXF-1L) with a maximum output power of 30 W and a spectral bandwidth of $\Delta\lambda_{\text{p}} \sim 2.5$ nm was employed. The optical fibers of both diodes had a diameter of 600 μm and a numerical aperture of $\text{NA} = 0.22$. The pump at 0.81 μm of the thin-disk crystal was performed with a pump module that realized 16 passes of the pump radiation through the laser medium. A second pump

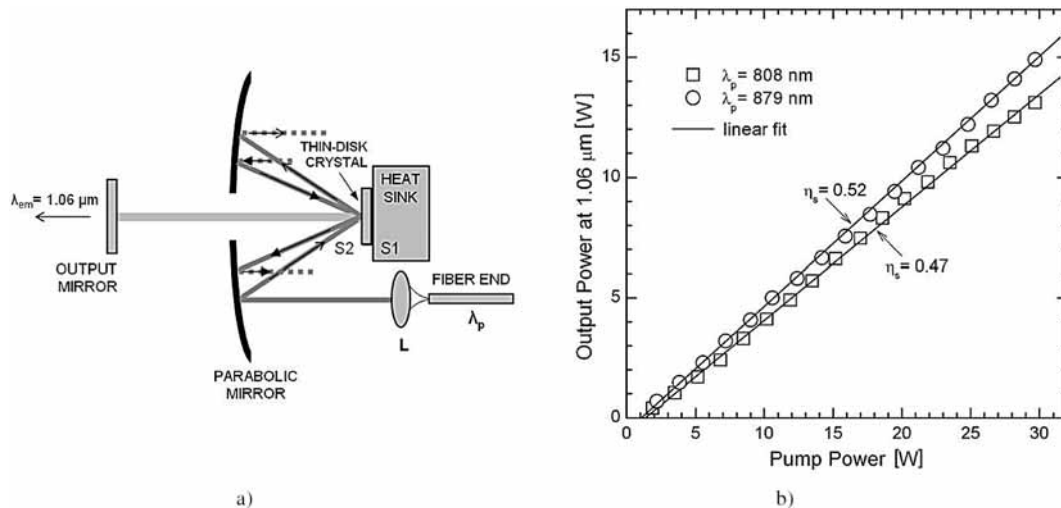


Fig. 9 – a) A sketch of a multi-pass pumped Nd-vanadate thin-disk laser; b) output power at 1.06 μm versus the pump power at 0.81 and 0.88 μm obtained from the Nd:GdVO₄ thin-disk crystal.

module with 24 passes was used for the pump at 0.88 μm . For both pump modules the pump-beam spot size on the laser media was 1.2 mm in diameter.

A linear resonator that was formed between side S1 of the thin-disk crystal and a concave output mirror with a radius of curvature of 300 mm was used for laser operation at 1.06 μm . Fig. 9b shows the cw output power delivered by the 0.5 at % Nd:GdVO₄ thin-disk laser with an output mirror of transmission $T = 0.028$. The pump at 808 nm with the 16 passes pump module delivered 13.1 W of output power at 1063 nm for 29.7 W of pump power. The optical efficiency η_o was 0.44 and the slope efficiency η_s was 0.47. About 97% of the 808 nm radiation was absorbed by the Nd:GdVO₄ crystal. In-band pumping at 879 nm improved these results. The Nd:GdVO₄ thin disk yielded 14.9 W of output power at 1063 nm with an optical efficiency $\eta_o = 0.50$ and a slope efficiency $\eta_s = 0.52$. The absorption efficiency at 879 nm was estimated to be $\eta_a \sim 0.93$.

The generation of green light at 0.53 μm was realized with a Z-type resonator, as shown in Fig. 10a. The radii of curvature of mirror M3 and M4 were 300 and 100 mm, respectively. Mirror M5 was plane. Distances S1-M3 and M3-M4 were equals (~ 250 mm) and the total resonator length was about 560 mm. Mirror M3 was HR coated at $\lambda_{em} = 1.06 \mu\text{m}$, and mirror M5 was HR coated at both λ_{em} and its second harmonic $\lambda_{2\omega} = 0.53 \mu\text{m}$. The visible radiation was coupled out through mirror M4 that was HR coated at λ_{em} and HT coated at 0.53 μm . The generation of green light was achieved with a 20 mm long LBO crystal that was cut for type I phase matching ($\theta = 90^\circ$, $\phi = 11.4^\circ$) at 25°C. The LBO crystal, which

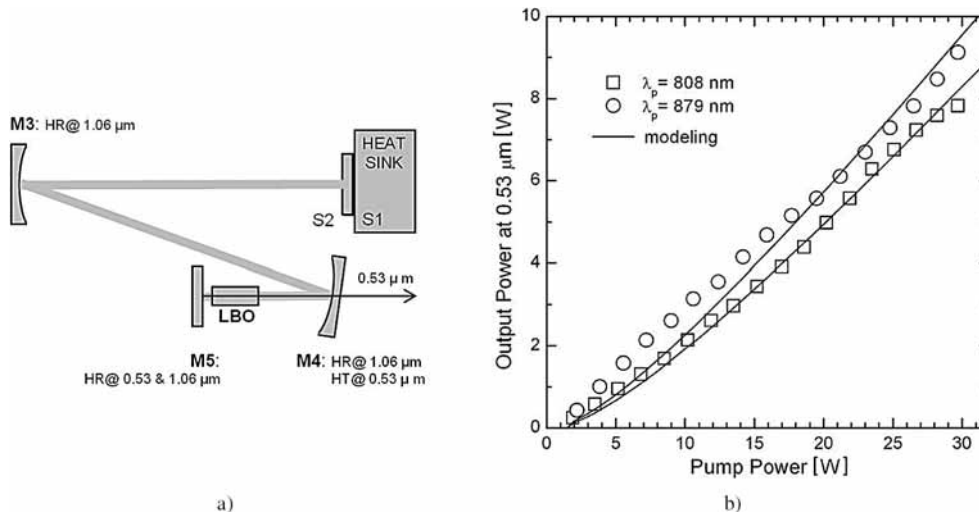


Fig. 10 – a) The Nd:GdVO₄ thin-disk laser intracavity frequency doubled by LBO nonlinear crystal; b) output power at 0.53 μm versus the pump power at 0.81 and 0.88 μm .

had both surfaces AR coated for λ_{em} and $\lambda_{2\omega}$, was inserted into the M4-M5 arm, close to mirror M5.

Fig. 10b presents the output power at 0.53 μm obtained from the intracavity frequency doubled Nd:GdVO₄ crystal. The Nd:GdVO₄ laser yielded green light with a maximum output power of 7.8 W under the pump at 808 nm with the 16 passes module. The overall efficiency η_o was 0.26. With the 24 passes pump module the Nd:GdVO₄ laser reached an output power at 0.53 μm of 9.1 W for the pump at 879 nm. The optical efficiency η_o was 0.31. Continuous lines of Fig. 10b are calculus of the output power on a model introduced by R.G. Smith [28].

The Nd:YVO₄ thin-disk laser had an output power of 11.4 W at 1064 nm for the pump at 808 nm, with an optical efficiency $\eta_o = 0.38$ and a slope efficiency $\eta_s = 0.42$. The absorption efficiency at 808 was evaluated to be $\eta_a \sim 0.95$. The pump with the 24 passes module could assure an absorption $\eta_a \sim 0.87$ of the 879 nm radiation. The output power at 1064 nm increased to 12.2 W with an optical efficiency η_o and a slope efficiency η_s of 0.41 and 0.42, respectively. In-band pumping into the ⁴F_{3/2} emitting level at 880 nm of the Nd:YVO₄ thin disk crystal yielded an output power of 8.5 W at 0.53 μm with an optical efficiency η_o of 0.29.

An 0.3 at % Nd:YVO₄ thin-disk crystal of 300 μm thickness was tested also for lasing at the 914 nm ⁴F_{3/2} \rightarrow ⁴I_{9/2} transition, under in-band pumping at 880 nm. A linear resonator (as shown in Fig. 9a) with an output mirror with $T = 0.1$ % at 914 nm was used in the experiments. The Nd:YVO₄ crystal yielded a maximum cw output power of 3.1 W at 914 nm when it was placed in the 24 passes pump module. For generation of deep blue light at 457 nm the authors used a Z-type folded cavity as presented in Fig. 10a, which was modified for $\lambda_{em} = 914$ nm and $\lambda_{2\omega} = 457$ nm [27]. The intracavity frequency doubling was obtained with a 15 mm long LBO nonlinear crystal (type I, $\theta = 90^\circ$, $\phi = 21.7^\circ$, 25°C). The maximum output power at 457 nm was 1.0 W under pumping with the same pump module. These results can be further improved by a proper choice of the laser and nonlinear crystals, and by an improved design of the folded cavity used for the generation of deep-blue light.

3. CONCLUSIONS

In conclusion, results obtained from Nd-based laser materials that were pumped directly into the ⁴F_{3/2} emitting level and that emitted at the fundamental wavelengths of 0.9, 1.06 and 1.3 μm were presented. Some of the discussed data

are records or first demonstrations of such kind of laser operation. Laser emission at 1.06 μm with slope efficiency close of the quantum defect ratio was achieved in end-pumped at 0.88 μm Nd:YAG and Nd-vanadate crystals using a tunable Ti:Sapphire laser as source of excitation. Efficient laser operation at 0.946 μm in Nd:YAG under pumping with a Ti:sapphire laser, and first demonstration of laser emission at 1.3 μm in Nd:YAG that was pumped with diode lasers at 0.88 μm were realized. These results proved that the laser emission parameters with respect to the absorbed power are enhanced by pumping resonantly into the emitting level.

A good absorption of the pump radiation was obtained by using highly-doped laser crystals with a thickness of a few millimeters in an end-pumping scheme, or thin-disk geometry of the laser crystal in a multi-pass pumping configuration. The first solution was used to demonstrate an intracavity frequency-doubled Nd:GdVO₄ laser that generated cw 5.1 W output power of green at 0.53 μm visible light under pumping with diode lasers at 0.81 μm . A multi-pass pumped Nd:GdVO₄ laser with a cw output power of 14.9 W at 1.06 μm and that generated 9.1 W of cw green light at 0.53 μm was also realized for the first time. Recent results obtained from a Nd:YAG laser [29], which delivered 250 W of cw output power at 1.06 μm with an absorbed pump power at 0.88 μm of 438 W, demonstrates clearly that the in-band pumping directly into the $^4\text{F}_{3/2}$ emitting level is a viable solution for performance improvements and further power scaling of solid-state lasers.

Acknowledgments. N. Pavel acknowledges research collaboration between the Laser Research Center of Institute for Molecular Science, Okazaki, Japan and Laboratory of Solid-State Quantum Electronics: During this collaboration the data reported for the end-pumping schemes were obtained. The author also acknowledges a post-doctoral scholarship of the Alexander von Humboldt Foundation, Bonn, Germany that allowed him to study at the Institute for Laser Physics of Hamburg University, Hamburg, Germany, where he investigated laser performances of the Nd-based thin-disk lasers. The Romanian Ministry of Science and Research supported partially this work through the CEEEX D07-27 project. The author would like to address a special “THANK YOU” to Prof. Dr. Voicu Lupei, for the guidance, help and support, encouraging and suggestions showed him since he was hired in the Laboratory of Solid-State Quantum Electronics (year 1990), and especially during the period spend together in Japan. These results would not be obtained without a major contribution of Prof. Dr. Voicu Lupei, and most of them are original contributions to the development of solid-state lasers.

REFERENCES

1. R. Newmann, *J. Appl. Phys.*, **34**, 2, 437 (1963).
2. M. Ross, *Proc. IEEE*, **56**, 2, 196–197 (1968).
3. L. J. Rosenkrantz, *J. Appl. Phys.*, **43**, 11, 4603–4605 (1972).
4. R. Lavi, S. Jackel, Y. Tzuk, M. Winik, E. Lebiush, M. Katz, I. Paiss, *Appl. Opt.*, **38**, 36, 7382–7385 (1999).
5. R. Lavi, S. Jackel, *Appl. Opt.*, **39**, 18, 3093–3098 (2000).

6. R. Lavi, S. Jackel, A. Tal, E. Lebiush, Y. Tzuk, S. Goldring, *Opt. Commun.*, **195**, 5–6, 427–430 (2001).
7. T. Kellner, C. Czeranowsky, G. Huber, *Laser operation of Nd:YVO₄ at 915 nm and 1064 nm under direct excitation of the upper laser manifold*, in: Tech. Digest of “Novel Lasers and Devices” Conference, Vol. **LTUD 2–1**, p. 107 (1999).
8. D. Dudley, N. Hodgson, H. Hoffman, F. Kopper, *Direct 880 nm diode-pumping of vanadates lasers*, in: Tech. Digest of “CLEO 2002” Conference, May 2002, California, USA, paper CTuI3.
9. V. Lupei, T. Taira, A. Lupei, N. Pavel, I. Shoji, A. Ikesue, *Appl. Phys. Lett.*, **79**, 5, 590–592 (2001).
10. V. Lupei, A. Lupei, S. Georgescu, T. Taira, Y. Sato, A. Ikesue, *Phys. Rev.*, B **64**, 092102 (2001).
11. V. Lupei, N. Pavel, T. Taira, *Opt. Lett.*, **26**, 21, 1678–1680 (2001).
12. K. K. Deb, R. G. Buser, J. Paul, *Appl. Opt.*, **20**, 7, 1203–1206 (1981).
13. T. Y. Fan, *IEEE J. Quantum Electron.*, **QE-29**, 6, 1457–1459 (1993).
14. I. Shoji, Y. Sato, S. Kurimura, V. Lupei, T. Taira, A. Ikesue, K. Yoshida, *Opt. Lett.*, **27**, 4, 234–236 (2002).
15. C. Czeranowsky, M. Schmidt, E. Heumann, G. Huber, S. Kutovoi, Y. Zavartsev, *Opt. Commun.*, **205**, 4–6, 361–365 (2002).
16. Y. Sato, T. Taira, N. Pavel, V. Lupei, *Appl. Phys. Lett.*, **82**, 6, 844–846 (2003).
17. V. Lupei, N. Pavel, T. Taira, *Appl. Phys. Lett.*, **83**, 18, 3653–3655 (2003).
18. V. Lupei, N. Pavel, Y. Sato, T. Taira, *Opt. Lett.*, **28**, 23, 2366–2368 (2003).
19. V. Lupei, N. Pavel, T. Taira, *Appl. Phys. Lett.*, **81**, 15, 2677–2679 (2002).
20. N. Pavel, V. Lupei, J. Saikawa, T. Taira, H. Kan, *Appl. Phys.*, B **82**, 4, 599–605 (2006).
21. N. Pavel, V. Lupei, T. Taira, *Opt. Express*, **13**, 20, 7948–7953 (2005).
22. N. Pavel, T. Taira, *IEEE J. Sel. Top. Quantum Electron.*, **11**, 3, 631–637 (2005).
23. A. Giesen, H. Hügel, A. Voss, K. Witting, U. Brauch, H. Opower, *Appl. Phys.*, B **58**, 5, 365–372 (1994).
24. A. Giesen, J. Speiser, *IEEE J. Sel. Top. Quantum Electron.*, **13**, 3, 598–609 (2007).
25. N. Pavel, T. Taira, *Opt. Commun.*, **260**, 1, 271–276 (2006).
26. N. Pavel, K. Lünstedt, K. Petermann, G. Huber, *Appl. Opt.*, **46**, 34, 8256–8263 (2007).
27. N. Pavel, C. Kränkel, R. Peters, K. Petermann, G. Huber, *Phys. B*, **91**, 3–4, 415–419 (2008).
28. R. G. Smith, *IEEE J. Quantum Electron.*, **QE-6**, 4, 215–223 (1970).
29. M. Frede, R. Wilhelm, D. Kracht, *Opt. Lett.*, **31**, 24, 3618–3619 (2006).